Pergamon

Geochimica et Cosmochimica Acta, Vol. 66, No. 22, pp. 4007–4014, 2002

0016-7037/02 $22.00 + .00

PII S0016-7037(02)00961-4

Coupled Ce–Nd isotope systematics and rare earth elements differentiation of the moon

MASAHARU TANIMIZU* and TSUYOSHI TANAKA

Department of Earth and Planetary Sciences, Graduate School of Science, Nagoya University, Chikusa, Nagoya 464-8602, Japan

(*Received September* 24, 2001; *accepted in revised form May* 14, 2002)

Abstract—$^{138}Ce/^{142}Ce$ and $^{143}Nd/^{144}Nd$ isotope ratios of lunar samples are determined to constrain the petrogenetic differentiation and evolution of the moon. High-precision Ce–Nd isotope data, well-defined Rb–Sr isochrons, and rare earth elements (REE) abundances of lunar samples show that unexpectedly low La/Ce ratios of evolved lunar highland samples are preserved from at least 3.9 Ga. Precise analysis of REE abundances indicates that the low La/Ce ratio results from a depletion of La relative to other REE. This depletion can be seen in pristine KREEP basalts and Mg-suite rocks from 3.85 to 4.46 Ga. As REE abundances of all these samples are controlled by the presence of a KREEP component, the depletion was probably inherited from a late crystallization sequence of the lunar magma ocean related to the production of the original KREEP component. *Copyright © 2002 Elsevier Science Ltd*

1. INTRODUCTION

The rare earth elements (REE), which have similar physical and chemical properties, have received considerable attention in geochemistry and cosmochemistry. These similar properties arise from the nature of their electronic configurations, leading to 3+ oxidation state and a small but steady decrease in ionic radius with increase in atomic number. The size differences account for the tendency of REE to substitute in different minerals with an affinity that is a smooth function of atomic number. The only exceptions are for Eu and Ce, which occur commonly as Eu^{2+} and Ce^{4+}, depending on oxygen fugacity. The predictable behavior of REE has led to their widespread use, typically presented as CI chondrite-normalized plots, to provide constraints on processes such as igneous rock petrogenesis, metamorphism, and rock weathering. Moreover, REE contain two long-lived decay systems, ^{147}Sm–^{143}Nd and ^{138}La–^{138}Ce, which give us information regarding rock ages and initial ratios. Applications of the La–Ce decay system is rare compared with the Sm–Nd system due to the difficulty of measuring Ce isotopes with high reproducibility; however, La–Ce isotopic data, particularly when combined with Sm–Nd systematics, are useful to elucidate evolution of light-REE (LREE: La, Ce, Pr, Nd, and Sm) (Tanaka et al., 1987). Figure 1 is a schematic figure which explains the relationship between LREE patterns of rocks derived from a chondritic uniform reservoir (CHUR) and directions of their isotopic growth of $^{138}Ce/^{142}Ce$ and $^{143}Nd/^{144}Nd$ ratios with time in ϵ units.

In this study, we report Ce isotopic results of lunar materials obtained using a newly developed Ce isotope analysis technique and the decay constant by Tanimizu (2000). Their Nd isotope ratios, REE abundances, and Rb–Sr mineral ages are also examined to discuss their source material, early differentiation process, and evolution of the interior.

* Author to whom correspondence should be addressed (mash@geo.titech.ac.jp).

Present address: Dept. of Earth and Planet. Sci., Grad. School of Sci. and Eng., Tokyo Institute of Technology, Ookayama 2-12-1, Meguro, Tokyo 152-8551, Japan.

2. ANALYTICAL PROCEDURE

Lunar samples investigated for this study are high Ti mare basalts (10017,334 and 75015,1), KREEP (a crustal component which is enriched in K, REE, P, and other incompatible elements) basalts (14310,578 and 65015,29), a basaltic fragment of a polymict breccia 14321 (14321,1490), and a soil 14163. The latter four samples originate from the lunar highland. After mineral separation with heavy liquids and a hand magnet, all powdered samples were decomposed by HF, $HClO_4$, and HNO_3. The samples 14163, 14310, and 75015 were aliquoted from solutions used in previous studies (Masuda et al., 1972; Tanaka et al., 1985; Tanaka et al., 1986). The following measurements were carried out from the obtained solutions: $^{138}Ce/^{142}Ce$ and $^{143}Nd/^{144}Nd$ isotope ratios of the whole rock samples together with $^{87}Sr/^{86}Sr$ isotope ratios of mineral separates; concentrations of LREE (La, Ce, Nd, and Sm), Rb, and Sr by stable isotope dilution mass spectrometry (ID–MS); all REE abundances using inductively coupled plasma source mass spectrometry (ICP–MS), except the mare basalt samples; major element compositions using inductively coupled plasma source atomic emission spectrometry (ICP–AES). The trace elements were refined by conventional column chemistry using HCl and 2-Methyllactic acid as elements. $^{138}Ce/^{142}Ce$, $^{143}Nd/^{144}Nd$, and $^{87}Sr/^{86}Sr$ ratios were measured with a thermal ionization mass spectrometer, VG Sector 54-30 equipped with seven Faraday cups and a recently introduced low noise digital voltmeter. Mass fractionations during the measurements were corrected with $^{140}Ce/^{142}Ce = 7.941$, $^{146}Nd/^{144}Nd = 0.7219$, and $^{86}Sr/^{88}Sr = 0.1194$. Decay constants used in this study are 2.32×10^{-12} yr^{-1} for ^{138}La to ^{138}Ce, 4.41×10^{-12} yr^{-1} for ^{138}La to ^{138}Ba (Tanimizu, 2000), 6.54×10^{-12} yr^{-1} for ^{147}Sm to ^{143}Nd, and 1.42×10^{-11} yr^{-1} for ^{87}Rb to ^{87}Sr (Steiger and E. Jäger, 1977), respectively.

3. RESULTS AND DISCUSSION

3.1. Rb–Sr Systematics

Results of Rb–Sr analyses of mineral separates are given in Table 1. The Rb–Sr data define internal isochron ages of 3.57 ± 0.03, 3.84 ± 0.11, 4.22 ± 0.23, and 3.90 ± 0.06 Ga for

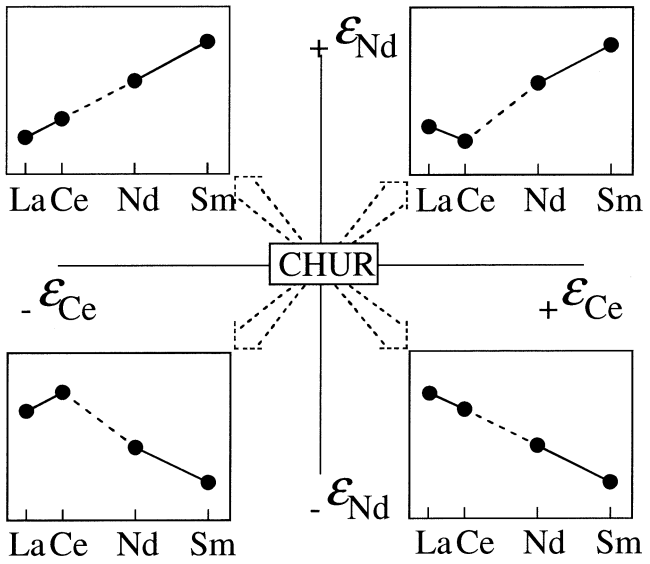

Fig. 1. A schematic figure which explains the relationship between LREE patterns of rocks derived from CHUR and directions of their isotopic growth of Ce and Nd isotope ratios in ϵ_{Ce} and ϵ_{Nd} values with time. The ϵ values are calculated from $\epsilon(T) = (R_{Sample}(T)/R_{CHUR}(T) - 1) \times 10^4$ where $R_{Sample}(T)$ and $R_{CHUR}(T)$ refer to the isotope ratio of $^{138}Ce/^{142}Ce$ or $^{143}Nd/^{144}Nd$ for a sample and a chondritic uniform reservoir (CHUR) at time T ($T = 0$ for present).

10017, 14310, 14321, and 65015, respectively (Figs. 2a–2d). These ages are consistent with previous Rb–Sr ages [3.51 ± 0.05 Ga for 10017 (Papanastassiou et al., 1970), 3.79 ± 0.04 and 3.75 ± 0.07 Ga for 14310 (Papanastassiou and Wasserburg, 1971; Tanaka et al., 1985), 4.03 ± 0.08 Ga for 14321 (Dasch et al., 1987), and 3.85 ± 0.02 Ga for 65015 (Papanastassiou and Wasserburg, 1972)]. The ages around 3.9 Ga, which are common in lunar highland breccias, are probably reequilibration ages caused by global impact metamorphism associated with formation of the major lunar basins (Nyquist and Shih, 1992). The relatively large uncertainties of their Rb–Sr ages compared to that of the mare basalt 10017 (Fig. 2) seem to be a consequence of slight incomplete reequilibration of their Rb–Sr isotope systematics around 3.9 Ga.

3.2. REE Abundances and Ce and Nd Isotope Ratios

REE data determined in this study are summarized in Tables 2–4 with those of reference rocks determined using the same procedure. REE concentrations were normalized to those of CI chondrite (Anders and Grevesse, 1989) with a slight modification in Tb, Ho, and Yb (M. Ebihara, private communication) (Fig. 3). The influence of neutron capture on ^{149}Sm was corrected using previously determined values (Russ et al., 1971;

Table 1. Rb–Sr data of mineral separates from lunar samples. Error limits which apply to the last digits are statistical error of 95% confidence interval. The uncertainty of $^{87}Rb/^{86}Sr$ is ±1%. The average value of a Sr isotope reference, NIST SRM 987, is 0.710250 ± 0.000011 (1 S.D.).

Sample	Fraction	Rb (ppm)	Sr (ppm)	$^{87}Rb/^{86}Sr$	$^{87}Sr/^{86}Sr$
10017	bulk	5.66	162	0.101	0.704 660 ± 14
	fine fraction	5.63	208	0.0783	0.703 448 ± 14
	pyroxene 1	4.16	83.6	0.144	0.706 816 ± 16
	pyroxene 2	4.18	80.4	0.150	0.707 223 ± 14
	pyroxene 3	2.15	56.3	0.111	0.705 126 ± 14
	ilmenite 1	10.3	119	0.251	0.712 523 ± 14
	ilmenite 2	9.66	109	0.257	0.712 751 ± 16
	plagioclase	2.30	541	0.0123	0.700 038 ± 14
	ρ: 2.85–3.15	7.91	301	0.0761	0.703 406 ± 14
75015	bulk	0.606	205	0.00857	0.699 695 ± 13
14310	fine fraction	13.3	207	0.186	0.710 775 ± 13
	pyroxene 1	23.3	209	0.323	0.718 393 ± 16
	pyroxene 2	21.5	121	0.515	0.729 211 ± 19
	pyroxene 3	2.77	28.2	0.284	0.716 018 ± 16
	plagioclase 1	5.26	286	0.0533	0.703 426 ± 15
	plagioclase 2	15.9	283	0.162	0.709 863 ± 13
	mixture	14.1	156	0.261	0.715 171 ± 16
14321	bulk	14.4	162	0.258	0.715 256 ± 16
	fine fraction	13.9	191	0.211	0.713 025 ± 14
	pyroxene 1	3.37	51.1	0.191	0.711 435 ± 14
	pyroxene 2	2.21	30.8	0.208	0.712 548 ± 16
	plagioclase	13.1	300	0.126	0.707 126 ± 18
	ρ: 3.15–3.33	9.64	117	0.239	0.714 676 ± 24
	ρ: 2.85–3.15	15.2	158	0.278	0.717 097 ± 17
	mixture 1	19.5	194	0.291	0.717 418 ± 14
	mixture 2	20.0	187	0.310	0.718 701 ± 14
	mixture 3	20.4	196	0.301	0.718 090 ± 16
	mixture 4	17.5	180	0.280	0.716 854 ± 14
65015	bulk	8.92	163	0.158	0.709 331 ± 14
	pyroxene	15.4	185	0.241	0.714 051 ± 14
	Fe spherule	15.5	163	0.275	0.715 987 ± 13
	plagioclase	12.3	243	0.146	0.708 559 ± 13
	ρ: 2.85–3.15	5.58	141	0.115	0.706 857 ± 24
	mixture	7.27	144	0.146	0.708 619 ± 14
14163	bulk	15.4	183	0.244	0.715 027 ± 16

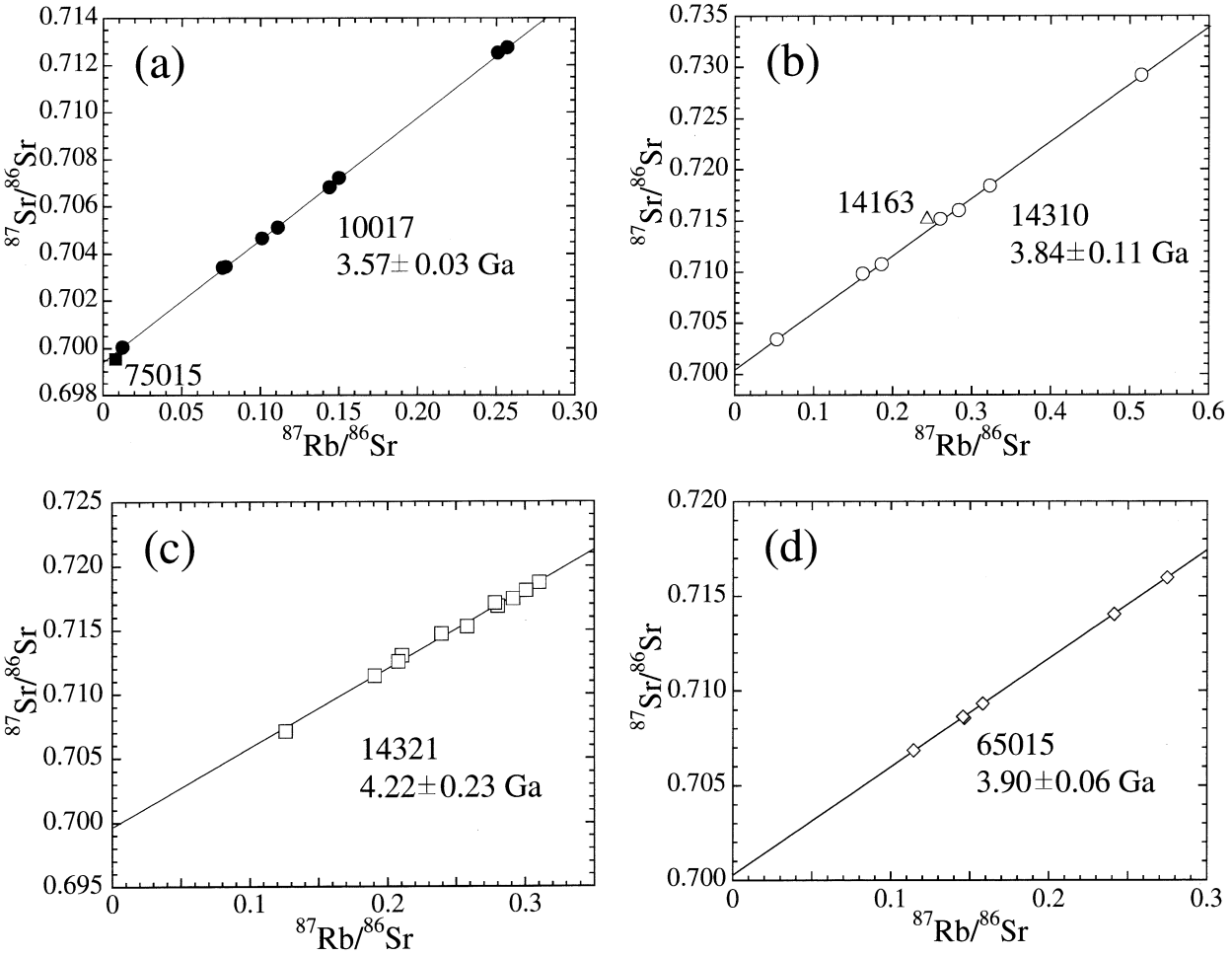

Fig. 2. Rb–Sr isochron diagram of (a) high Ti basalts, 10017 and 75015, (b) a KREEP basalt 14310 and a soil 14163, (c) a fragment from a polymict breccia, 14321, and (d) a KREEP basalt, 65015. Mineral separates of 10017, 14310, 14321, and 65015 define internal isochron ages corresponding to 3.57 ± 0.03, 3.84 ± 0.11, 4.22 ± 0.23, and 3.90 ± 0.06 Ga with initial $^{87}Sr/^{86}Sr$ ratios of 0.69940 ± 0.00003, 0.7005 ± 0.0002, 0.6996 ± 0.0008, and 0.7003 ± 0.0001, respectively. These are consistent with previous Rb–Sr results (Papanastassiou et al., 1970; Papanastassiou and Wasserburg, 1971; Papanastassiou and Wasserburg, 1972; Tanaka et al., 1985; Dasch et al., 1987). The age of the basaltic fragment 14321,1490 is one of the oldest ages of 14321 (Dasch et al., 1987) with highest REE content and initial $^{87}Sr/^{86}Sr$ ratio. The chemical composition of the fragment is almost identical to those of typical KREEP basalts.

Lugmair and Carlson, 1978; Nyquist et al., 1995). As shown in Fig. 3, unexpectedly low La/Ce ratios were recognized in the LREE-enriched evolved lunar highland samples (14310, 14321, 65015, and 14163) in contrast to straight LREE enrichment patterns of the terrestrial rocks.

Present $^{138}Ce/^{142}Ce$ and $^{143}Nd/^{144}Nd$ isotope ratios of investigated samples are plotted in Figure 4 in ϵ units. The two LREE-depleted mare basalts from A11 and A17 sites plot in the second quadrant, as expected from Figure 1. In contrast, the four LREE-enriched crustal samples have near-zero ϵ_{Ce} values with negative ϵ_{Nd} values. If the low La/Ce ratios of these samples are the result of erroneously high Ce contents, then Ce* concentrations should give the true values. This is an estimated Ce content interpolated between La and Nd in REE pattern (see Table 2). If the Ce* values are correct, then the four LREE-enriched samples would have evolved in the fourth quadrant (Fig. 1) along the calculated path indicated in Fig. 4 from La/Ce* ratios in Table 3. However, it is evident that the four samples are not on this path, having near-zero ϵ_{Ce} values (Fig. 4). This is in contrast with the Ce–Nd isotopic result of terrestrial LREE-enriched crustal rocks (Bushveld gabbro in this study and crustal rocks in Tanaka et al., 1987), which obviously plot in the fourth quadrant. This contrast is due to the extremely low La/Ce ratios of the lunar highland samples in comparison to the straight-line LREE enrichment of the terrestrial samples (Fig. 3). If the low La/Ce ratios were formed secondarily by some recent event without disturbing the Rb–Sr decay system, then the Ce and Nd isotope ratios would have plotted in the fourth quadrant. Based on this observation, it is obvious that low La/Ce ratios are commonly present in LREE-enriched lunar highland samples, not as artifacts in laboratories, and they have not been generated by recent events. Some nondestructive REE determinations of lunar highland samples by INAA confirm the existence of the low La/Ce ratio (e.g., Palme et al., 1978).

Because the Rb–Sr results from mineral separates yield

Table 2. REE concentrations of lunar samples in ppm with major element compositions in percent. Ce* concentrations were calculated from CI chondrite-normalized values with an equation of $Ce^*/Ce_{CI} = ((La_{Sample}/La_{CI})^2 \times (Nd_{Sample}/Nd_{CI}))^{(1/3)}$.

	10017,334	75015,1	14310,578	14321,1490	65015,29	14163	Eucrite Camel Donga	Terrestrial rock Bushveld gabbro	Ref. rock BCR-1
La	24.8	6.19	49.5	73.6	58.4	68.7	3.71	2.73	
Ce	72.8	22.4	131.1	192.6	152.9	181.2	9.71	5.55	
Nd	57.1	24.5	76.6	116.5	94.6	107.6	7.37	2.91	
Sm	19.7	10.4	21.7	32.8	26.5	30.3	2.37	0.722	
Ce*			118.2	177.1	141.6	164.7			
La			49.1	73.5	58.1	70.1			24.9
Ce			126.9	191.4	151.8	183.0			53.2
Pr			17.1	25.8	20.6	24.6			6.68
Nd			77.8	118.1	96.0	112.7			29.1
(Pm)									
Sm			20.9	32.3	26.0	30.9			6.70
Eu			2.33	2.45	1.99	2.59			1.92
Gd			24.4	38.0	30.8	36.5			6.68
Tb			4.14	6.43	5.13	6.14			1.00
Dy			27.8	43.5	34.5	41.5			6.25
Ho			5.64	8.95	7.06	8.55			1.26
Er			16.8	26.4	20.5	25.1			3.61
Tm			2.35	3.69	2.83	3.53			0.508
Yb			15.1	24.2	18.3	22.9			3.29
Lu			2.10	3.34	2.53	3.18			0.483
Y			140	216	173	207			32.7
TiO_2	12.4	9.45	0.9	1.9	1.3	1.8			
Al_2O_3	7.6	9.8	22.0	14.6	19.6	17.6			
FeO	19.4	18.1	6.3	11.7	8.1	10.1			
MgO	7.0	5.9	6.1	10.2	8.8	8.6			
CaO	10.1	11.7	12.3	9.4	11.8	10.5			
K_2O	0.31	0.04	0.71	0.67	0.42	0.68			

well-defined isochrons with no evidence of isotopic alteration, the Rb–Sr ages can be used to calculate initial ϵ_{Ce} and ϵ_{Nd} values (Table 4; Fig. 5). The following crystallization ages were used for the calculation: 3.75 Ga for 75015 (Paces et al., 1991), 4.56 Ga for 14163 (model age), 4.56 Ga for Camel Donga (Hirata, 2001), and 2.04 Ga for Bushveld gabbro (Tanimizu, 2000). The initial Ce–Nd isotopic data of the two mare basalts (10017 and 75015) are clearly distinct from each other (Fig. 5), indicating a difference in LREE patterns of their source materials. The LREE pattern of the 75015 source material must be more depleted than that of the 10017 (Tanaka et al., 1987). The four LREE-enriched lunar samples have near-zero initial ϵ_{Ce} values similar to their present-day values. All isotopic results indicate that the low La/Ce ratios were inherited by the time these rocks closed to Rb–Sr isotopic decay.

3.3. Interpretation of the Low La/Ce Ratio in Lunar Highland Samples

These low La/Ce ratios of lunar highland samples were reported by a few investigators (Masuda et al., 1972; Tanaka et al., 1985; Tanaka et al., 1986) and in our preliminary report (Tanimizu and Tanaka, 2001), and have been interpreted as positive Ce anomalies due to the presence of Ce^{4+}. However, based on an experimental study of iron–cerium interactions in silicate melts (Schreiber et al., 1980), it is difficult to produce

Table 3. La–Ce and Sm–Nd isotopic result of lunar samples. The uncertainty of $^{138}La/^{142}Ce$ is about ±0.5%. Error limits apply to the last digits. The average values ± 1 S.D. of Nd and Ce isotope references, La Jolla Nd, JNdi-1, and JMC304, are 0.511854 ± 0.000003, 0.515211 ± 0.000005, and 0.0225891 ± 0.0000013 (for 250 ratios), respectively.

	$^{147}Sm/^{144}Nd$	$^{143}Nd/^{144}Nd$	$^{138}La/^{142}Ce$	$^{138}Ce/^{142}Ce$	$^{138}La/^{142}Ce^*$
10017 bulk	0.2085 ± 9	0.513 065 ± 8	0.002 779	0.022 5822 ± 11	
75015 bulk	0.2558 ± 12	0.514 458 ± 7	0.002 254	0.022 5793 ± 11	
14310 fine fraction	0.1708 ± 12	0.511 788 ± 7	0.003 080	0.022 5864 ± 11	0.003 420
14321 bulk	0.1703 ± 11	0.511 823 ± 8	0.003 106	0.022 5852 ± 11	0.003 395
65015 bulk	0.1695 ± 8	0.511 810 ± 7	0.003 103	0.022 5853 ± 12	0.003 368
14163 bulk	0.1701 ± 9	0.511 834 ± 8	0.003 093	0.022 5866 ± 12	0.003 406
Camel Donga	0.1923 ± 13	0.512 587 ± 6	0.003 122	0.022 5853 ± 27	
Bushveld gabbro	0.1501 ± 4	0.511 656 ± 7	0.004 018	0.022 5920 ± 9	

Table 4. ϵ_{Ce} and ϵ_{Nd} values of lunar samples. Epsilon values were calculated using CHUR values of $^{138}Ce/^{142}Ce = 0.0225858$, $^{138}La/^{142}Ce = 0.003063$, $^{143}Nd/^{144}Nd = 0.512638$, and $^{147}Sm/^{144}Nd = 0.1966$ (Makishima and Masuda, 1993). Their original $^{138}Ce/^{142}Ce$ CHUR value was modified to our value by measuring the same Ce isotopic standard JMC304.

	$\epsilon_{Ce}(0)$	$\epsilon_{Nd}(0)$	$\epsilon_{Ce}(T)$	$\epsilon_{Nd}(T)$	$\epsilon_{Ce}(4.56\ Ga)$
10017 bulk	−1.59 ± 0.49	+8.33	−0.54 ± 0.54	+2.88 ± 0.82	
75015 bulk	−2.90 ± 0.49	+35.50	+0.50 ± 0.53	+6.78 ± 1.08	
14310 fine fraction	+0.27 ± 0.49	−16.57	+0.20 ± 0.55	−3.83 ± 1.10	+0.19 ± 0.56
14321 bulk	−0.27 ± 0.49	−15.90	−0.46 ± 0.56	−1.57 ± 1.11	−0.47 ± 0.56
65015 bulk	−0.22 ± 0.53	−16.15	−0.38 ± 0.60	−2.51 ± 0.80	−0.41 ± 0.61
14163 bulk	+0.35 ± 0.53	−15.69	+0.21 ± 0.61	−0.18 ± 1.00	+0.21 ± 0.61
Camel Donga	−0.22 ± 1.20	−1.00	−0.50 ± 1.27	+1.42 ± 1.36	−0.50 ± 1.27
Bushveld gabbro	+2.75 ± 0.40	−19.16	+1.01 ± 0.40	−7.15 ± 0.20	

Ce^{4+} in an anhydrous lunar basaltic system. A precise determination of monoisotopic Pr abundance, which cannot be measured with ID–MS, is one of the keys to evaluate the presence of Ce anomalies. ICP–MS is suitable for this purpose, though analytical uncertainty of REE determination by ICP–MS, about ±3%, is larger than that of ID–MS, typically within ±1%. As shown in Figure 3, most current La, Ce, and Nd data of ICP–MS agree with those of ID–MS within ±3% (Table 2). The Pr abundances of the lunar highland samples are all on tie lines of Ce and Nd, not of La and Nd in the REE patterns. Therefore, it is more likely that the low La/Ce ratio is a relative depletion of La to other REE.

Was the La depletion inherited from lunar precursor materials or produced during the early igneous evolution of the moon? Because the investigated samples experienced resetting events at approximately 3.9 Ga, we cannot establish an upper limit on the timing of the La depletion based on our data. As many lunar highland samples are metamorphosed by the impact brecciation, it is necessary to examine REE patterns of pristine lunar samples with known ages determined by ID–MS. Precisely determined REE patterns of two KREEP basalts, 15386 and 72275 (Hubbard et al., 1974), two Mg-suite rocks (norite and troctolite), 15445 and 76535 (Ridley et al., 1973; Haskin et al., 1974), and an anorthosite 60025 (Nakamura et al., 1973) are shown in Figure 6. A ferroan anorthosite 60025, which is among the first crustal rocks produced by the lunar magma ocean with a Sm–Nd mineral age of 4.44 ± 0.02 Ga (Carlson and Lugmair, 1988), has a straight LREE pattern (Nakamura et al., 1973). In contrast, the evolved lunar highland rocks, two KREEP basalts and two Mg-suite rocks, have slight La depletions with younger Sm–Nd mineral ages of 3.85 ± 0.08 and 4.08 ± 0.07 Ga for the KREEP basalts (Carlson and Lugmair, 1979; Shih et al., 1992) and 4.26 ± 0.06 and 4.46 ± 0.07 Ga for the Mg-suite rocks (Lugmair et al., 1976; Shih et al., 1993).

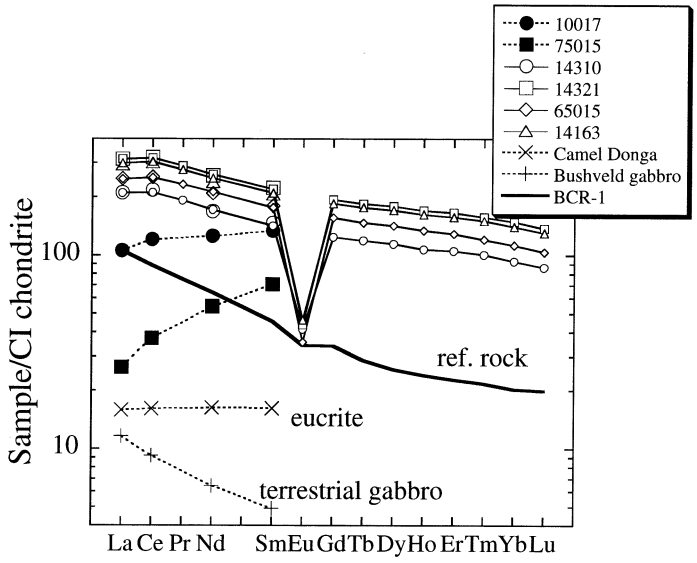

Fig. 3. REE patterns of lunar highland samples (open symbols) and mare basalts (solid symbols) with those of eucrite and terrestrial rocks. The REE concentrations are normalized to those of CI chondrite (0.2347, 0.6032, 0.0891, 0.4524, 0.1471, 0.0560, 0.1966, 0.0363, 0.2427, 0.0556, 0.1589, 0.0242, 0.1625, and 0.0243 from La to Lu except Pm in ppm; Anders and Grevesse, 1989) with a modification of Tb (0.0348 ppm), Ho (0.0525 ppm), and Yb (0.0234 ppm) (M. Ebihara, private communication). Large symbols were determined with ID–MS, whereas small symbols connected by solid lines were done by ICP–MS. The two data sets are almost consistent within the analytical uncertainty. Unexpectedly low La/Ce ratios are recognized in all LREE-enriched lunar samples as well as steep negative Eu anomalies in contrast to straight-line LREE enrichment patterns of terrestrial rocks.

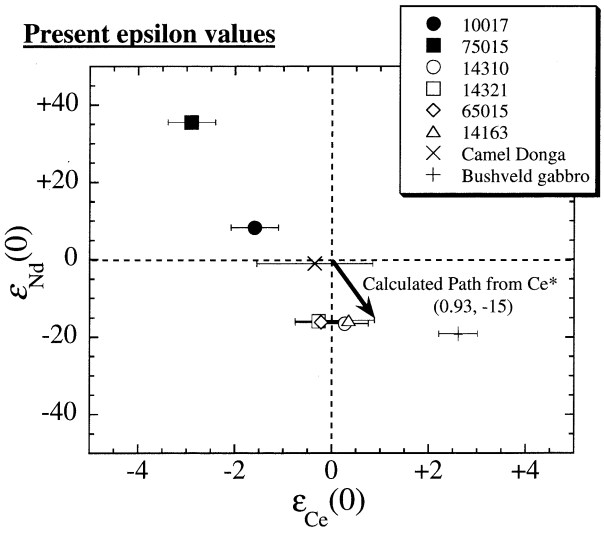

Fig. 4. Present ϵ_{Ce}–ϵ_{Nd} diagram of investigated samples. The ϵ notation is the isotopic deviation of a sample from a chondritic uniform reservoir (CHUR) in parts in 10^4. A solid arrow is a calculated isotopic evolution path from CHUR for 4.56 Ga with $^{138}La/^{142}Ce^* = 0.00340$ and $^{147}Sm/^{144}Nd = 0.170$. LREE-enriched lunar samples have ϵ_{Ce} values lower than this isotopic evolution path. This means that the low La/Ce ratios have been preserved for a long time. Ce* is calculated by the interpolation of La and Nd in REE pattern (see Table 2).

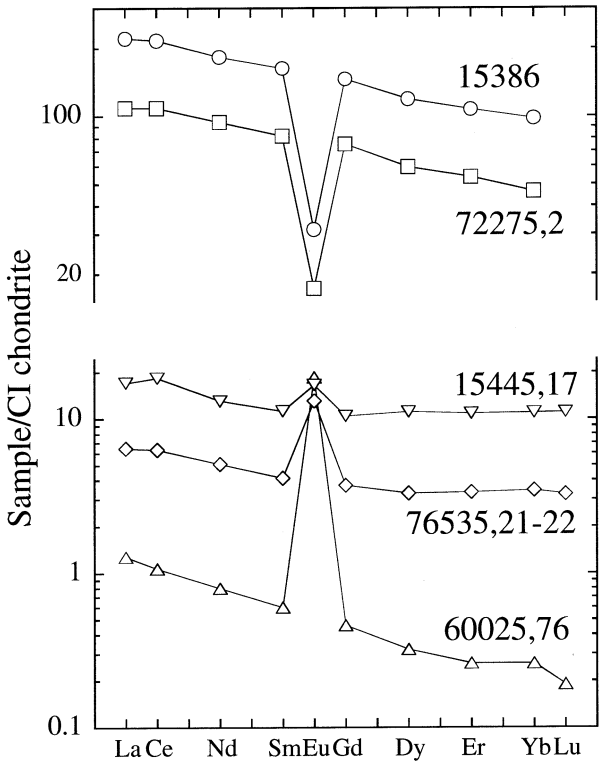

Fig. 6. REE patterns of pristine lunar highland rocks determined by ID–MS (Nakamura et al., 1973; Ridley et al., 1973; Haskin et al., 1974; Hubbard et al., 1974). Relative depletions of La are recognized in KREEP basalts (15386 and 72275), norite (15445), and troctolite (76535). A straight-line LREE pattern of an anorthosite (60025), which is among the first crustal rocks, suggests that the lunar magma ocean had a straight LREE pattern at the liquidus phase of plagioclase.

The crystallization ages of Mg-suite rocks, which are considered as the products of the post-magma ocean highland magmatism, are younger than those of anorthosites (Nyquist and Shih, 1992). These rocks are generated by decompression melting of early lunar magma ocean cumulates, followed by the assimilation of original KREEP component, which is the residuum of the lunar magma ocean (Shearer and Papike, 1999). KREEP basalts were formed by a similar process, but with a higher proportion of the KREEP component (Warren, 1988; Neal and Taylor, 1989). From this fact, REE patterns of these evolved lunar highland rocks shown in Figure 6 reflect that of the original KREEP component. Therefore, their REE patterns and crystallization ages suggest that the lunar magma ocean originally had a straight LREE pattern at least before crystallization of plagioclase, and the depletions of La were generated during a later stage of crystallization of the lunar magma ocean, related to the production of the original KREEP component.

The La depletion can be explained as a consequence of mineral crystallization which favors La from the melt, before the production of the original KREEP component. Plagioclase is the first candidate, because its partition coefficients increase gradually from Lu to La except for the higher compatibility of Eu (Phinney and Morrison, 1990). The steep negative Eu anomalies of KREEP basalts support the separation of plagioclase from the melt. In this case, the La depletion might be also recognized in later magma ocean cumulates with negative Eu anomalies, though the LREE-depleted signature of almost all other lunar components prevents this. Alternatively, a minor

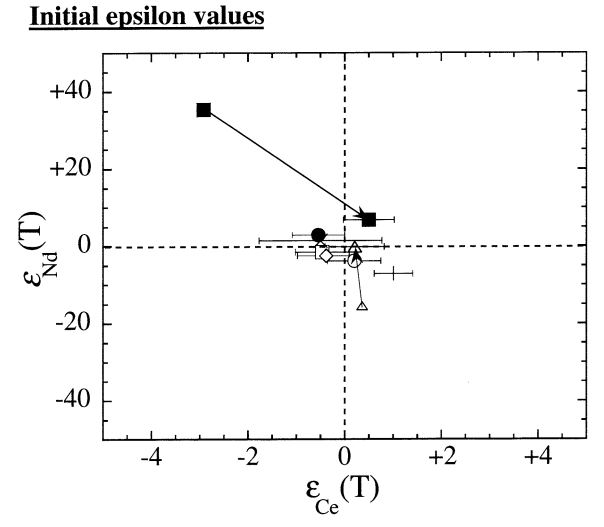

Fig. 5. Calculated initial ϵ values of investigated samples with CHUR values of $^{138}La/^{142}Ce = 0.003063$ and $^{147}Sm/^{144}Nd = 0.1966$ (Makishima and Masuda, 1993). Mare basalts from A11 and A17 evolved in the second quadrant depending on the degrees of LREE depletion of their source materials, which were inherited from the primary crystallization of the lunar magma ocean. LREE-enriched lunar samples have near-zero ϵ_{Ce} values similar to their present-day values. Exact radiometric ages are not determined for 75015 and 14163. The age dependences of their initial ϵ values are expressed with arrows from $\epsilon(0)$ to $\epsilon(3.75\ Ga)$ for 75015 and from $\epsilon(0)$ to $\epsilon(4.56\ Ga)$ for 14163, respectively. Symbols are the same as in Figure 4.

but relatively REE concentrated Ca-phosphate phase may control the REE pattern related to the production of the original KREEP component itself (Jolliff et al., 1993).

The approximate differentiation time of the original KREEP component is estimated to be around 4.4 Ga from model ages of KREEP basalts (Nyquist and Shih, 1992). La–Ce model ages should be consistent with these ages, if the La depletion was inherited from the crystallization sequence of the lunar magma ocean. Unfortunately, present Ce isotope data are not of sufficient precision to prove this. These data only show that even at the formation age of the solar system, the ϵ_{Ce}(4.56 Ga) values of the evolved lunar highland samples do not deviate from $\epsilon_{Ce} = 0$ within analytical uncertainty (Table 4). On the basis of the Ce isotope data alone, the La depletion of the investigated samples could have been generated at the time of the melting event that led to their eruption on the surface. However, the La depletion of old pristine Mg-suite rocks discussed above and almost constant La/Ce ratios of investigated samples (Table 3) can be explained well by assuming the low La/Ce ratio of the original KREEP component.

The combination of Ce–Nd isotope systematics of lunar samples provides an argument that the original KREEP component is depleted in La relative to other REE. The relative depletion of La, a common feature of evolved lunar highland rocks, can be utilized as an indicator to survey assimilation of the KREEP component into various lunar samples. It could also provide fertile new information for understanding the crystallization sequence of the lunar magma ocean that led to the production of a KREEP residual liquid. Although a similar depletion of La has not been recognized in terrestrial ancient crustal rocks, the presence of an LREE-enriched alkali basaltic crust at a very early stage is proposed to explain positive initial ϵ_{Nd} values of archean mantle derived rocks (Galer and Goldstein, 1991). Further investigation of Ce–Nd isotope systematics of pristine lunar rocks and archean terrestrial rocks might provide significant information about the style of the terrestrial magma ocean and a basis for comparing igneous evolution of the moon and the earth. This systematics will also contribute to age determinations of metamorphic rocks with Ce anomalies. As REE patterns are important to evaluate the origin and history of geochemical samples, La–Ce isotope systematics will gain increasing importance in geochemistry.

Acknowledgments—The authors thank K. Yamamoto, M. Takebe, and F. Yamashita, Nagoya Univ. for their technical support on ICP–MS analysis. We have benefited greatly from discussion with I. Kawabe, Nagoya Univ. We are indebted to T. J. Fagan, C. Drăguşanu, and K. Shibata for their patience in revising this paper. Thoughtful review by H. Palme has enhanced the quality of this paper. This research was supported in part by the Japan Society for the Promotion of Science for Young Scientists (10003537) and by the 31st Kurata Scholarship.

Associate editor: H. Palme

REFERENCES

Anders E. and Grevesse N. (1989) Abundances of the elements: Meteoritic and solar. *Geochim. Cosmochim. Acta* **53,** 197–214.

Carlson R. W. and Lugmair G. W. (1979) Sm–Nd constraints on early lunar differentiation and the evolution of KREEP. *Earth Planet. Sci. Lett.* **45,** 123–132.

Carlson R. W. and Lugmair G. W. (1988) The age of ferroan anorthosite 60025: Oldest crust on a young Moon? *Earth Planet. Sci. Lett.* **90,** 119–130.

Dasch E. J., Shih C.-Y., Bansal B. M., Wiesmann H., and Nyquist L. E. (1987) Isotopic analysis of basaltic fragments from lunar breccia 14321: Chronology and petrogenesis of pre-Imbrium mare volcanism. *Geochim. Cosmochim. Acta* **51,** 3241–3254.

Galer S. J. G. and Goldstein S. L. (1991) Early mantle differentiation and its thermal consequences. *Geochim. Cosmochim. Acta* **55,** 227–239.

Haskin L. A., Shih C.-Y., Bansal B. M., Rhodes J. M., Wiesmann H., and Nyquist L. E. (1974) Chemical evidence for the origin of 76535 as a cumulate. *Proc. Lunar Sci. Conf.* **5,** 1213–1225.

Hirata T. (2001) Determinations of Zr isotopic composition and U-Pb ages for terrestrial and extraterrestrial Zr-bearing minerals using laser ablation-inductively coupled plasma mass spectrometry: implications for Nb-Zr isotopic systematics. *Chem. Geol.* **176,** 323–342.

Hubbard N. J., Rhodes J. M., Wiesmann H., Shih C.-Y., and Bansal B. M. (1974) The chemical definition and interpretation of rock types returned from the non-mare regions of the moon. *Proc. Lunar Sci. Conf.* **5,** 1227–1246.

Jolliff B. L., Haskin L. A., Colson R. O., and Wadhwa M. (1993) Partitioning in REE-saturating minerals: Theory, experiment, and modelling of whitlockite, apatite, and evolution of lunar residual magmas. *Geochim. Cosmochim. Acta* **57,** 4069–4094.

Lugmair G. W., Marti K., Kurtz J. P., and Scheinin N. B. (1976) History and genesis of lunar troctolite 76535. *Proc. Lunar Sci. Conf.* **7,** 2009–2033.

Lugmair G. W. and Carlson R. W. (1978) The Sm–Nd history of KREEP. *Proc. Lunar Sci. Conf.* **9,** 689–704.

Makishima A. and Masuda A. (1993) Primordial Ce isotopic composition of the solar system. *Chem. Geol.* **106,** 197–205.

Masuda A., Nakamura N., Kurasawa H., and Tanaka T. (1972) Precise determination of rare-earth elements in the Apollo 14 and 15 samples. *Proc. Lunar Sci. Conf.* **3,** 1307–1313.

Nakamura N., Masuda A., Tanaka T., and Kurasawa H. (1973) Chemical compositions and rare-earth features of four Apollo 16 samples. *Proc. Lunar Sci. Conf.* **4,** 1407–1414.

Neal C. R. and Taylor L. A. (1989) Metasomatic products of the lunar magma ocean: The role of KREEP dissemination. *Geochim. Cosmochim. Acta* **53,** 529–541.

Nyquist L. E. and Shih C.-Y. (1992) The isotopic record of lunar volcanism. *Geochim. Cosmochim. Acta* **56,** 2213–2234.

Nyquist L. E., Wiesmann H., Bansal B., Shih C.-Y., Keith J. E., and Harper C. L. (1995) ^{146}Sm–^{142}Nd formation interval for the lunar mantle. *Geochim. Cosmochim. Acta* **59,** 2817–2837.

Paces J. B., Nakai S., Neal C. R., Taylor L. A., Halliday A. N., and Lee D.-C. (1991) A strontium and neodymium isotopic study of Apollo 17 high-Ti mare basalts: Resolution of ages, evolution of magmas, and origins of source heterogeneities. *Geochim. Cosmochim. Acta* **55,** 2025–2043.

Palme H., Baddenhausen H., Blum K., Cendales M., Dreibus G., Hofmeister H., Kruse H., Palme C., Spettel B., Vilcsek E., Wanke H., and Kurat G. (1978) New data on lunar samples and achondrites and a comparison of the least fractionated samples from the earth, the moon, and the eucrite parent body. *Proc. Lunar Sci. Conf.* **9,** 125–157.

Papanastassiou D. A., Wasserburg G. J., and Burnett D. S. (1970) Rb–Sr ages of lunar rocks from the Sea of Tranquility. *Earth Planet. Sci. Lett.* **8,** 1–19.

Papanastassiou D. A. and Wasserburg G. J. (1971) Rb–Sr ages of igneous rocks from the Apollo 14 mission and the age of the Fra Mauro formation. *Earth Planet. Sci. Lett.* **12,** 36–48.

Papanastassiou D. A. and Wasserburg G. J. (1972) Rb–Sr systematics of Luna 20 and Apollo 16 samples. *Earth Planet. Sci. Lett.* **17,** 52–63.

Phinney W. C. and Morrison D. A. (1990) Partition coefficients for calcic plagioclase: Implications for Archean anorthosites. *Geochim. Cosmochim. Acta* **54,** 1639–1654.

Ridley W. I., Hubbard N. J., Rhodes J. M., Wiesmann H., and Bansal B. (1973) The petrology of lunar breccia 15445 and petrogenetic implications. *J. Geol.* **81,** 621–631.

Russ, G. P., III, Burnett D. S., Lingenfelter R. E., and Wasserburg G. J. (1971) Neutron capture on ^{149}Sm in lunar samples. *Earth Planet. Sci. Lett.* **13,** 53–60.

Schreiber H. D., Lauer H. V., and Thitinant T. (1980) The redox state of cerium in basaltic magmas: an experimental study of iron–cerium interactions in silicate melts. *Geochim. Cosmochim. Acta* **44,** 1599–1612.

Shearer C. K. and Papike J. J. (1999) Magmatic evolution of the Moon. *Amer. Mineral.* **84,** 1469–1494.

Shih C.-Y., Nyquist L. E., Bansal B. M., and Wiesmann H. (1992) Rb–Sr and Sm–Nd chronology of an Apollo 17 KREEP basalt. *Earth Planet. Sci. Lett.* **108,** 203–215.

Shih C.-Y., Nyquist L. E., Dasch E. J., Bogard D. D., and Wiesmann H. (1993) Ages of pristine noritic clasts from breccias 15445 and 15455. *Geochim. Cosmochim. Acta* **57,** 915–931.

Steiger R. H. and Jäger E. (1977) Subcommission on geochronology: Convention on the use of decay constants in geo- and cosmochemistry. *Earth Planet. Sci. Lett.* **36,** 359–362.

Tanaka T., Shimizu H., Shibata K., and Masuda A. (1985) Positive cerium anomaly of lunar 14310: examination by ^{138}Ce/^{142}Ce. *Lunar Planet. Sci.* **16,** 847–848.

Tanaka T., Shimizu H., Shibata K., and Masuda A. (1986) Water in ancient moon?: possible oxic alteration of 14310. *Lunar Planet. Sci.* **17,** 867–868.

Tanaka T., Shimizu H., Kawata Y., and Masuda A. (1987) Combined La–Ce and Sm–Nd isotope systematics in petrogenetic studies. *Nature* **327,** 113–117.

Tanimizu M. (2000) Geophysical determination of the ^{138}La β^- decay constant. *Phys. Rev. C* **62,** 017601.

Tanimizu M. and Tanaka T. (2001) Ce–Nd–Sr isotope systematics of eucrites and lunar rocks. In *Origin of Elements in the Solar System* (ed. O. Manuel), pp. 555–572. Kluwer, Academic/Plenum.

Warren P. H. (1988) The origin of pristine KREEP: Effects of mixing between urKREEP and the magmas parental to the Mg-rich cumulates. *Proc. Lunar Planet. Sci. Conf.* **18,** 233–241.